

Activation of Sphingolipid Pathway in the Livers of Lipodystrophic *Agpat2*^{-/-} Mice

Shireesha Sankella,^{1,2} Abhimanyu Garg,^{1,2} and Anil K. Agarwal^{1,2}

¹Division of Nutrition and Metabolic Diseases, University of Texas Southwestern Medical Center, Dallas, Texas 75390; and ²Center for Human Nutrition, University of Texas Southwestern Medical Center, Dallas, Texas 75390

A several fold increase in triacylglycerol is observed in the livers of lipodystrophic *Agpat2*^{-/-} mice. We have previously reported an unexpected increase in the phosphatidic acid (PA) levels in the livers of these mice and that a few specific molecular species of PA were able to transcriptionally upregulate hepatic gluconeogenesis. In the current study, we measured the metabolites and expression of associated enzymes of the sphingolipid synthesis pathway. The entire sphingolipid pathway was activated both at the gene expression and the metabolite level. The levels of some ceramides were increased by as much as ~eightfold in the livers of *Agpat2*^{-/-} mice. Furthermore, several molecular species of ceramides were increased in the plasma of *Agpat2*^{-/-} mice, specifically ceramide C16:0, which was threefold elevated in the plasma of both the sexes. However, the ceramides failed to increase glucose production in mouse primary hepatocytes obtained from wild-type and *Agpat2*^{-/-} mice, further establishing the specificity of PA in the induction of hepatic gluconeogenesis. This study shows elevated levels of sphingolipids in the steatotic livers of *Agpat2*^{-/-} mice and increased expression of associated enzymes for the sphingolipid pathway. Therefore, this study and those in the literature suggest that ceramide C16:0 could be used as a biomarker for insulin resistance/type 2 diabetes mellitus.

Copyright © 2017 Endocrine Society

This article has been published under the terms of the Creative Commons Attribution Non-Commercial, No-Derivatives License (CC BY-NC-ND; <https://creativecommons.org/licenses/by-nc-nd/4.0/>).

Freeform/Key Words: ceramides, AGPAT, lipodystrophy, hepatic steatosis, diabetes mellitus

The 1-acylglycerol-3-phosphate *O*-acyltransferase 2 knockout (*Agpat2*^{-/-}) mouse was generated based on the genetic observations that we made in human subjects with congenital generalized lipodystrophy, type 1 [1]. *Agpat2*^{-/-} mice recapitulate all the features of human lipodystrophy, including hyperinsulinemia, diabetes mellitus, hypertriglyceridemia, and hepatic steatosis [2]. The AGPAT2 enzyme converts lysophosphatidic acid (LPA) to phosphatidic acid (PA) [3]. PA is a precursor for several phospholipids and neutral lipids. Livers of these mice are engorged with lipids, including phospholipids and neutral lipids. We have also reported a several fold increase in hepatic triacylglycerol levels in *Agpat2*^{-/-} mice [2].

Currently, 11 AGPAT isoforms are known, both in humans and mice, encoded by different genes with different tissue expression patterns [4]. Some of these AGPATs have additional acyltransferase activities. For example, AGPAT10 is reported to have glycerol phosphate acyltransferase activity [5]. Similarly, AGPAT8 and AGPAT9 also possess lysocardiolipin acyltransferase 1 [6, 7] and lysophosphatidylcholine acyltransferase 1 [8] activity, respectively. Although almost all of these AGPATs have been studied to define their substrate specificities and subcellular localizations [4], only AGPAT1 and AGPAT2 isoforms are more widely studied. AGPAT1 and AGPAT2 isoforms are close homologs [3], but their tissue expression patterns are different: AGPAT1 is ubiquitously expressed, whereas AGPAT2 is more tissue-restricted [3]. *In vitro* substrate specificities for the AGPAT1 and

Abbreviations: CerS, ceramide synthase; DMEM, Dulbecco's modified Eagle medium; HPLC, high-performance liquid chromatography; LC-MS/MS, liquid chromatography-tandem mass spectrometry; LPA, lysophosphatidic acid; PA, phosphatidic acid; RT-qPCR, quantitative reverse transcriptase polymerase chain reaction; WT, wild-type.

Received 23 March 2017

Accepted 15 May 2017

First Published Online 18 May 2017

July 2017 | Vol. 1, Iss. 7

doi: 10.1210/js.2017-00157 | Journal of the Endocrine Society | 980–993

AGPAT2 recombinant proteins are very similar, with few differences [3]. Both the enzymes prefer *sn*-1-C18:1-LPA and C18:1-coenzyme A as acyl acceptor and donor, respectively [3]. However, AGPAT1 may also use odd-chain acyl-coenzyme A (C15:0) as donor [3].

In a previous report, we measured the hepatic levels of LPA and PA in *Agpat2*^{-/-} mice [9]. Although the LPA levels were elevated as expected, surprisingly we also found the PA levels to be increased. We also showed that some specific molecular species of PA increase hepatic gluconeogenesis when tested in cultured mouse primary hepatocytes. This increased hepatic gluconeogenesis is due to the transcriptional activation of glucose-6-phosphatase (*G6pase*) and phosphoenolpyruvate carboxykinase (*Pepck*) enzymes [9].

In the steatotic liver, lipids of all classes are increased, which includes phospholipids such as LPA, PA, phosphatidylcholine, and phosphatidylethanolamine; neutral lipids such as monoacylglycerol, diacylglycerol, and triacylglycerol; and sphingolipids such as ceramides [10]. Previous studies have reported increased ceramide levels in the livers of *ob/ob* mice [10, 11]. In seipin-deficient *Bscl2*^{-/-} mice, another mouse model of lipodystrophy, the total hepatic ceramide levels were lower upon 4-hour fasting compared to those of nonfasting mice [12]. The pathway for the synthesis of sphingolipid, including ceramide and its metabolites, is shown in Fig. 1. The synthesis of sphingolipids is a complex process and requires >28 distinct enzymes [14, 15]. Since the livers of *Agpat2*^{-/-} mice have increased *de novo* lipogenesis (fatty acid synthesis), it seems likely that some of the synthesized fatty acids might condense with the amino acid serine, the first and rate-limiting step in the *de novo* sphingolipid biosynthetic pathway.

In this study, we analyzed several metabolite groups and various associated enzymes of the sphingolipid biosynthesis pathway in the plasma and livers of *Agpat2*^{-/-} and wild type mice. Moreover, we tested whether the elevated ceramide levels increase glucose output in cultured mouse primary hepatocytes.

1. Materials and Methods

A. Animals

The development and phenotype of *Agpat2*^{-/-} mice have been reported previously [2]. These mice are of mixed genetic background (C57B6/S129Sv) and were maintained in a pathogen-free environment, constant temperature, and were fed *ad libitum* a regular chow diet and kept in a 12-hour light–dark cycle. All animal studies were approved by the Institutional Use and Care of Animals and BioSafety Committee at the University of Texas Southwestern Medical Center, Dallas, TX.

B. Sphingolipid Extraction

Total sphingolipids were extracted as follows: 40 mg flash-frozen liver from 4-month-old mice was homogenized in 2.0 mL organic extraction solvent (isopropanol:water:ethyl acetate, 25:10:65; v:v:v). Immediately afterward, 20 μ L internal standard solution was added. The mixture was vortexed and sonicated in an ultrasonic bath for 40 minutes at 40°C. Next, the samples were allowed to reach room temperature, and 1.5 mL aqueous sucrose buffer (25 mM, pH 7.0) was added. Two-phase liquid extraction was performed, the supernatant was transferred to a new tube, and the pellet was re-extracted. Supernatants were combined and evaporated under nitrogen. The dried residue was reconstituted in 200 μ L high-performance liquid chromatography (HPLC) solvent B (methanol/formic acid 99:1; v:v containing 5 mM ammonium formate) for liquid chromatography-tandem mass spectrometry (LC-MS/MS) analysis. Plasma samples were processed using a similar methodology requiring 25 μ L sample.

C. Sphingolipid Quantification

Quantitative analysis of sphingolipids was achieved by LC-MS/MS electrospray ionization using selective reaction monitoring scan mode. Lipid separation was achieved by reverse-phase

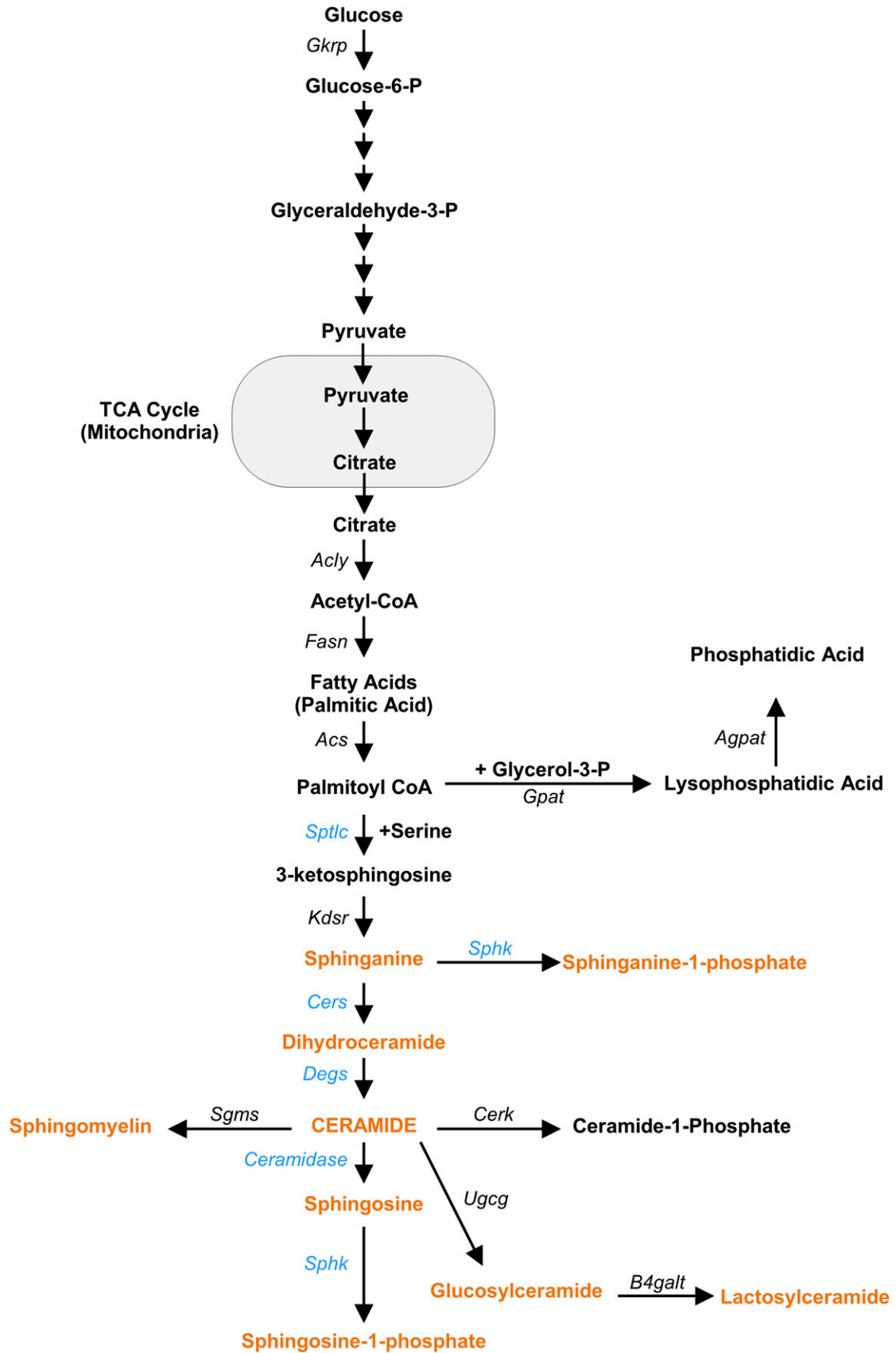


Figure 1. Lipogenesis, sphingolipid, and PA synthesis pathways. Glucose is the main intracellular substrate for the generation of fatty acids (FA). In the livers of *Agpat2*^{-/-} mice, there is an increase of *de novo* lipogenesis [2]. Shown are some of the key steps involved in the conversion of glucose to FAs (reviewed in [13]). The fate of FAs most likely depends on their intracellular concentrations and could enter different pathway(s), including glycerophospholipid synthesis or the sphingolipid synthesis pathway. In sphingolipid synthesis, first palmitoyl Co-A condenses with the amino acid serine to generate 3-ketosphingosine, which is then reduced to form sphinganine. In the next two sequential steps, ceramide synthase converts sphinganine to dihydroceramide, followed by its conversion by desaturase to ceramide. Further modifications of ceramide are also depicted. In glycerophospholipid synthesis, glycerol-3-phosphate is acylated to produce LPA and an additional acylation to generate PA. The enzymes of these pathway are as follows: *Spltc*, serine palmitoyltransferase; *Kdsr*, 3-ketosphingosine reductase; *Sphk*, sphingosine kinase (note *Sphk* has much broader substrate specificity phosphorylating both sphinganine and sphingosine); *CerS*, ceramide synthase; *Degs*, dihydroceramide desaturase; *Sgms*, sphingomyelin synthase; *Cerk*, ceramide kinase; *Ugcg*, UDP-glucose ceramide hexosyltransferase or hexosylceramide synthase; *B4galt*, UDP-Gal:betaGlcNAc β 1,4-galactosyltransferase or lactosylceramide synthase. Most of the enzymes for this pathway have multiple isoforms; for example, *CerS* has six known isoforms. Key enzymes for *de novo* lipogenesis: *Gkrp*, glucokinase regulatory protein; *Acyl*, ATP citrate lyase; *Fasn*, fatty acid synthase; *Acs*, Acyl-coenzyme A synthetase; TCA cycle, tricarboxylic acid cycle. Key enzymes for glycerophospholipid synthesis: *Gpat*, glycerol-3-phosphate acyltransferase; *Agpat*, 1-acylglycerol-3-phosphate *O*-acyltransferase. Those metabolites shown in orange and those enzymes shown in blue were measured in this study.

liquid chromatography on a 2.1 (internal diameter) \times 150-mm Kinetex C8, 2.6- μ m core-shell particle (Phenomenex, Torrance, CA) column under a gradient elution over 20 minutes, using three different mobile phases, as follows: eluent A consisting of CH₃OH/H₂O/HCOOH, 58/41/1, v/v/v with 5 mM ammonium formate; eluent B consisting of CH₃OH/HCOOH, 99/1, v/v with 5 mM ammonium formate; and eluent C consisting of CH₃OH/CH₂Cl₂ 35/65, v/v with 5 mM ammonium formate. Gradient description: 0 minutes, 60% A, 40% B, 0.5% C, hold for 1 minute; 4 minutes, 25% A, 75% B, 0% C; 13 minutes, 100% B, hold for 3 minutes; 16 minutes 100% C, hold for 2 minutes; 18 minutes, 60% A, 40% B, 0% C. The instrument consisted of a Shimadzu Prominence HPLC system equipped with a CBM-20A controller, a DGUA3 degasser, three HPLC solvent delivery modules LC-ADX, a CTO-20 AC column oven/chiller maintained at 30°C, and a SIL-20ACTHTautosampler. The HPLC system is coupled to an API 5000 LC-MS/MS mass spectrometer (AB SCIEX, Framingham, MA) equipped with a Turbo V ion source operating the electrospray ionization probe in positive mode. The concentration of each metabolite was determined according to calibration curves using the peak–area ratio of analyte vs corresponding internal standard [16–19]. Calibration curves were generated using serial dilutions of each target analyte. The mass/charge ratios (*m/z*) and retention time for each of the metabolites are presented in Supplemental Table 1, and product ion scans for representative metabolites for each class are presented in Supplemental Fig. 1(A) and 1(B). Sphingolipid standards and the Internal Standard Cocktail Mix II were purchased from Avanti Polar Lipids (Alabaster, AL). C22:0 hexosylceramide was purchased from Matreya (Pleasant Gap, PA). This analysis was carried out at University of Texas Southwestern Metabolic Phenotyping Core Facility.

D. Preparation of Liposomes With Ceramides and Transfection of Primary Mouse Hepatocytes

Liposomes were prepared fresh for each experiment, as described earlier [9]. A total of 100 μ M various ceramides and 0.1 μ Ci [³H]-oleoyl-LPA (PerkinElmer, Waltham, MA) was dried and resuspended in phosphate-buffered saline. Our previous data show that LPA has no effect on glucose production from hepatocytes [9]. The mixture was sonicated for 15 minutes, and the liposomes were used in cell culture experiments. Control cells received the liposomes without the ceramides.

E. Isolation of Mouse Primary Hepatocytes

Primary hepatocytes were isolated from 1-month-old nonfasted mice of both sexes by a two-step collagenase perfusion method as described earlier [9, 20, 21]. Briefly, mice were anesthetized with isoflurane, and a catheter (24 × 3/4" safelet catheter; Fisher Scientific, Waltham, MA) was inserted in the portal vein. The liver was perfused with the liver perfusion medium (Life Technologies, Carlsbad, CA) maintained at 37°C using a peristaltic pump at a rate of 3 mL/min until the liver blanched. The liver was then perfused with the liver digest medium (Life Technologies) at a rate of 3 mL/min for 20 minutes, excised from the animal, and placed in a petri dish containing the liver digest media at 37°C. Hepatocytes were released by removing the hepatic capsule and then passed through 100 μm cell strainer. The cells were washed three times in low-glucose Dulbecco's modified Eagle medium (DMEM) containing 100 mM HEPES by centrifuging at 25g for 2 minutes at 4°C. The cell pellet was resuspended in low-glucose DMEM containing 10% fetal bovine serum and 1% antibiotics. Approximately 1 × 10⁶ cells were seeded into each well of a collagen-coated six-well plate (Fisher Scientific) and allowed to attach overnight. The following day, cells were prepared for glucose output assay.

F. DNA Extraction

Approximately 50 mg liver from 4-month-old wild-type (WT) or *Agpat2*^{-/-} mice was homogenized in 100 mM Tris-HCl, pH 7.5, containing 10 mM NaCl. Cellular debris was removed by centrifugation at 3000g for 5 minutes at 4°C, and an aliquot was used to extract DNA. DNA was extracted with Easy-DNA kit (Invitrogen, Carlsbad, CA) following the manufacturer's protocol.

G. Glucose Output Assay

Glucose output was measured, as described previously [9]. Briefly, hepatocytes isolated from the livers of 1-month-old WT or *Agpat2*^{-/-} mice were plated on collagen-coated six-well plates and allowed to attach overnight. Cells were starved for 1 hour by incubating in phenol red-free, glucose-free DMEM (Sigma-Aldrich, St. Louis, MO). Cells were incubated in media containing sodium pyruvate and sodium lactate for 6 hours. Before the end of 6 hours, the cells were incubated with 100 μM PA (C16:0/18:1), used in this study as a positive control, or 100 μM ceramides C16:0, C18:0, or C24:1 for 30 minutes. Culture media was collected, and glucose was measured using a colorimetric assay kit from Cayman Chemical (Ann Arbor, MI). The glucose output was normalized to cellular protein content. Protein concentration was determined by a commercially available colorimetric assay (Bio-Rad Laboratories, Hercules, CA).

H. Quantitative Reverse Transcriptase Polymerase Chain Reaction (RT-qPCR) in Livers of WT and *Agpat2*^{-/-} Mice

Total RNA was extracted from mouse livers (100–200 mg) using RNA STAT-60 (Tel-Test, Friendswood, TX). Total RNA, in equal quantity, was pooled from six livers of each genotype and sex, and RT-qPCR was carried out in a 20 μL reaction volume. A total of 20 μg RNA was DNase I treated using the DNase-free kit from Ambion (Grand Island, NY). Complementary DNA was made using 2 μg DNase I-treated RNA using reverse-transcription kit from ABI (Carlsbad, CA). RT-qPCR was performed in duplicate using 2.5 μM primers, 20 ng complementary DNA, and SYBR Green. All RT-qPCR were carried out in 96-well plates using the StepOnePlus real-time polymerase chain reaction system (Applied Biosystems, Foster City, CA). RT-qPCR was performed three times and in duplicate, and the transcript levels were normalized to cyclophilin. The ΔC_t value for each sample was calculated as $\Delta C_t = [C_t (\text{gene of interest}) - C_t (\text{cyclophilin})]$. The $\Delta\Delta C_t$ value for each gene of interest was calculated as $\Delta\Delta C_t = [\Delta C_t (\textit{Agpat2}^{-/-}) - \Delta C_t (\text{WT})]$. The fold change was calculated as fold change = $2^{-\Delta\Delta C_t}$.

Primers used for gene amplification were obtained from Harvard primer bank [22–24] and Integrated DNA Technologies (Coralville, IA). Primers used are listed in Table 1.

I. Administration of Myriocin in *Agpat2*^{-/-} Mice

The 17.5-week-old *Agpat2*^{-/-} mice of both sexes were administered 0.5 mg/kg myriocin or vehicle every other day for 14 days by subcutaneous injection. The myriocin was prepared in 25% dimethyl sulfoxide, 25% propylene glycol, and 50% phosphate-buffered saline. Animals were killed at the end of the experiment, plasma was collected by cardiac puncture, and glucose was measured.

J. Statistical Analysis

Values are given as mean ± standard error of the mean or mean ± standard deviation. Statistical significance was calculated by two-tailed Student *t* test using GraphPad Prism version 6.04 for Windows. A *P* value ≤0.05 was considered statistically significant.

2. Results

A. Increased Levels of Sphingolipids in the Livers of Both Sexes of 4-Month-Old *Agpat2*^{-/-} Mice

As shown in Table 2, we observed a robust increase in the levels of several sphingolipid subspecies in both sexes of *Agpat2*^{-/-} mice compared with WT. The increases ranged from twofold to a robust increase of up to ~18- to 22-fold, but this increase was noticed only in the livers of male mice. Female mice showed an increase of ~one- to fivefold. This sexual dimorphism was expected because hepatic steatosis is more severe in male mice [2]. Most of the monitored sphingolipid species were found to be elevated in *Agpat2*^{-/-} mice livers. Ceramide

Table 1. Primers Used in This Study

Gene	GenBank Accession No.	PrimerBank ID	Forward Primer	Reverse Primer
<i>Sptlc1</i>	NM_009269.2	29244577a1	ACGAGGCTCCAGCATACCAT	TCAGAACGCTCCTGCAACTTG
<i>Sptlc2</i>	NM_011479.4	6755656a1	AACGGGGAAGTGAGGAACG	CAGCATGGGTGTTTCTTCAAAAAG
<i>Sptlc3</i>	NM_175467.3	28202041a1	TCTGAACGACAGTGCCTTAC	ATGCCTTCTATTTGCTGGG
<i>CerS1</i>	NM_138647.3	20149718a1	CCACCACACATCTTTTCGG	GGAGCAGGTAAGCGCAGTAG
<i>CerS2</i>	NM_029789	—	Mm.PT.58.10718121 from Integrated DNA Technologies	
<i>CerS3</i>	NM_001164201.1	255958166c1	CAGGCGAGGAGTATCCTGTG	CTCTCCGACCAGAACCATTTTC
<i>CerS4</i>	NM_026058.4	31541930a1	TACCACATCAGACCCCTGAAT	TGAAGTCCCTGCGTTTGACATC
<i>CerS5</i>	NM_028015.2	21312638a1	CGGGGAAAGGTGCTAAGGAT	GTTTCATGCAGTTGGCACCATT
<i>CerS6</i>	NM_172856.3	27370296a1	GATTCATAGCCAAACCATGTGCC	AATGCTCCGAACATCCCAGTC
<i>Degs1</i>	NM_007853.4	6681175a1	GAATGGGTCTACACGGACCAG	CGAGAAGCATCATGGCTACAA
<i>Degs2</i>	NM_001171002.1	27754029a1	AGCGACTTCGAGTGGGTCTA	TCCCCGTACTAACCAGCAGG
<i>Asah1</i>	NM_019734.3	9790019a1	CGTGGACAGAAGATTGCAGAA	TGGTGCCTTTTGACCAATAAT
<i>Asah2</i>	NM_018830.1	9055168a1	GCAAAGCGAACCTTCTCCAC	ACTGGTAACAAACAAGAGGGTGA
<i>Acer1</i>	NM_175731.4	28376625a1	TCTGAGGTGGATTGGTGTGAG	TGAGGGGTCCAAAGATGAGGA
<i>Acer2</i>	NM_139306.3	21314858a1	TGTGGCATATTTCTCATCTGCCT	CAATAAAAGCCCATTTCTCGCTG
<i>Acer3</i>	NM_025408.2	21313584a1	TGTGATTCACCTGAGGAACCTTCG	AGAAACTTCACCTTTGGCCTGTA
<i>Sphk1</i>	NM_011451	3659692a1	AAAATACTGAGAACTCGGTCCG	GCATCGCTTCTAAAGTCCAGA
<i>Sphk2</i>	NM_020011	31981070a1	CACGGCGAGTTTGGTTCCTA	CTTCTGGCTTTGGGCGTAGT
<i>Sgpl1</i>	NM_009163.4	31543694a1	CTGAAGGACTTCGAGCCTTATTT	ACTCCACGCAATGAGCTGC

All the primers were from Harvard PrimerBank (HPB) except *CerS2*, which was a pre-designed primer from Integrated DNA Technologies (Coralville, IA). The HPB primers were validated by amplification plots and dissociation curves, and analyzed on 2% agarose gel analysis, sequencing, and BLAST analysis.

Abbreviations: *Acer*, alkaline ceramidase; *Asah1*, acid ceramidase; *Asah2*, nonlysosomal ceramidase; *CerS*, ceramide synthase; *Degs*, dihydroceramide desaturase; *Sgpl*, sphingosine 1-phosphate lyase; *Sphk*, sphingosine kinase; *Sptlc*, serine palmitoyltransferase.

Table 2: Sphingolipid Pathway Metabolite Levels in the Livers of Wild Type (WT) and *Agpat2*^{-/-} Mice.

Name	Males				Females			
	Liver (pg/μg DNA)				Liver (pg/μg DNA)			
	WT (n = 6)	<i>Agpat2</i> ^{-/-} (n = 6)	Fold Change	P Value	WT (n = 6)	<i>Agpat2</i> ^{-/-} (n = 6)	Fold Change	P Value
	Mean ± SD	Mean ± SD			Mean ± SD	Mean ± SD		
Sphinganine	1.53 ± 0.27	4.37 ± 1.54 ^a	2.86 ^b	<0.01	1.98 ± 0.23	5.22 ± 2.09 ^a	2.64 ^b	0.01
Sphinganine 1P	0.63 ± 0.15	3.19 ± 1.43 ^a	5.06^c	<0.01	0.93 ± 0.10	3.37 ± 0.97 ^a	3.62^c	<0.01
Deoxy sphinganine	0.18 ± 0.04	1.07 ± 0.74 ^a	5.94 ^b	0.03	0.23 ± 0.01	1.15 ± 0.35 ^a	5.00 ^b	<0.01
DHC16:0	0.08 ± 0.02	0.27 ± 0.14 ^a	3.38 ^b	0.02	0.17 ± 0.03	0.28 ± 0.09 ^a	1.65 ^b	0.01
DHC18:0	0.12 ± 0.02	0.87 ± 0.62 ^a	7.25 ^b	0.03	0.56 ± 0.18	0.89 ± 0.37 ^a	1.59	0.03
DHC 24:0	0.90 ± 0.28	1.30 ± 0.75	1.44	0.27	1.03 ± 0.11	0.88 ± 0.32	-1.17	0.60
DHC 24:1	1.97 ± 0.41	5.97 ± 2.92 ^a	3.03 ^b	0.02	3.50 ± 0.11	5.75 ± 2.16	1.64 ^b	0.01
SM 16:0	519.28 ± 69.29	1799.03 ± 1114.97 ^a	3.46 ^b	0.04	829.97 ± 177.88	2131.58 ± 780.92 ^a	2.57 ^b	<0.01
SM 18:0	69.62 ± 13.13	561.88 ± 403.31 ^a	8.07 ^b	0.03	248.59 ± 78.62	623.81 ± 164.58 ^a	2.51	<0.01
SM 24:0	758.66 ± 281.60	678.38 ± 537.07	-1.12	0.75	826.84 ± 177.82	650.98 ± 266.62	-1.27	0.21
SM 24:1	976.91 ± 354.31	3105.95 ± 1871.75 ^a	3.18 ^b	0.04	1668.29 ± 347.37	3277.25 ± 1153.51 ^a	1.96 ^b	0.02
Cer16:0	1.26 ± 0.34	9.76 ± 5.83 ^a	7.75 ^c	0.02	2.30 ± 0.55	10.40 ± 2.50 ^a	4.52^c	<0.01
Cer18:0	0.36 ± 0.05	6.80 ± 3.25 ^a	18.89^c	<0.01	1.75 ± 0.61	8.00 ± 2.13 ^a	4.57^c	<0.01
Cer20:0	7.68 ± 1.48	20.89 ± 10.75 ^a	2.72 ^b	0.03	5.52 ± 1.38	17.46 ± 4.35 ^a	3.16 ^b	<0.01
Cer22:0	72.74 ± 4.99	90.56 ± 48.24	1.24	0.41	31.13 ± 5.29	78.29 ± 24.84 ^a	2.51 ^b	<0.01
Cer24:0	78.27 ± 19.86	140.34 ± 90.59	1.79	0.16	68.95 ± 6.04	94.23 ± 40.29	1.37	0.26
Cer24:1	82.72 ± 11.84	356.45 ± 156.74 ^a	4.31 ^b	<0.01	100.57 ± 17.59	322.47 ± 108.60 ^a	3.21 ^b	<0.01
HexCer-16:0	14.47 ± 7.12	39.01 ± 33.78	2.70	0.14	22.32 ± 2.33	40.14 ± 20.18 ^a	1.80 ^b	0.04
HexCer-18:0	0.39 ± 0.14	8.92 ± 6.00 ^a	22.87^c	0.02	6.09 ± 2.00	17.35 ± 9.77 ^a	2.85^c	0.03
HexCer-22:0	105.41 ± 16.45	136.05 ± 107.20	1.29	0.52	80.95 ± 21.50	115.91 ± 56.80	1.43	0.10
HexCer-24:1	26.63 ± 6.49	100.48 ± 58.98 ^a	3.77 ^b	0.03	47.06 ± 5.29	115.50 ± 47.64 ^a	2.45 ^b	<0.01
LacCer-16:0	7.50 ± 2.11	22.00 ± 11.68 ^a	2.93 ^b	0.03	6.95 ± 1.39	25.33 ± 12.13 ^a	3.64 ^b	<0.01
LacCer-24:0	7.19 ± 3.45	14.81 ± 8.07	2.06	0.07	6.57 ± 1.41	13.36 ± 6.39 ^a	2.03 ^b	0.02
Sphingosine	7.72 ± 1.36	22.23 ± 14.45	2.88	0.06	8.14 ± 0.78	23.60 ± 7.97 ^a	2.90 ^b	<0.01
Sphingosine 1P	2.29 ± 0.72	12.21 ± 5.78 ^a	5.33 ^b	<0.01	3.17 ± 0.83	12.05 ± 4.33 ^a	3.80 ^b	<0.01
Deoxy sphingosine	0.019 ± 0.006	0.04 ± 0.03	2.11	0.14	0.01 ± 0.00	0.048 ± 0.01 ^a	4.80 ^b	<0.01

Shown are the mean ± SD, fold change, and *P* value for metabolites of the sphingolipid synthesis pathway in the livers of *Agpat2*^{-/-} mice compared with those of WT mice.

Abbreviations: Cer, ceramide; DHC, dihydroceramide; HexCer, hexosylceramide; LacCer, lactosylceramide; SD, standard deviation; SM, sphingomyelin; sphinganine-1P, sphinganine-1-phosphate; sphingosine 1P, sphingosine-1-phosphate.

^aStatistically significant increases.

^bStatistically significant increase in *Agpat2*^{-/-} when compared with WT.

^cIncreased in both liver and plasma of both sexes of *Agpat2*^{-/-} mice and are statistically significant. Those in bold represent significant increase in both sexes.

C16:0 increased ~eightfold and C18:0 increased ~19-fold in males, but only ~two- to fivefold in female mice. Other notable increases were found for HexCer-C18:0 (~23-fold) and sphingosine 1-phosphate (~fivefold). In females, HexCer-C18:2 increased by ~threefold and sphingosine by ~fourfold. This suggests that the entire sphingolipid biosynthetic pathway is activated in the livers of *Agpat2*^{-/-} mice.

*B. Increased Levels of Sphingolipids in the Plasma of Both Sexes of 4-Month-Old *Agpat2*^{-/-} Mice*

We also observed a general elevation of sphingolipids in the plasma of *Agpat2*^{-/-} mice (Table 3). However, these increases were not as pronounced as those observed in liver. Ceramide C16:0, C18:0, HexCer-C18:0, and sphingosine-1-phosphate were found to be increased ~three- to eightfold. Two previous studies also observed an increase in ceramide C16:0 in the liver, as well as in the white and brown adipose tissues in murine models of ceramide synthase (CerS) deficiency [25, 26]. A CerS isoform 2 (CerS2) haploinsufficient mouse model resulted in a compensatory increase in the hepatic ceramide C16:0, resulting in diet-induced steatohepatitis and insulin resistance [26]. Deletion of CerS isoform 6 (CerS6) either globally (*CerS6*^{-/-}), or tissue specifically in brown adipose tissue

Table 3: Sphingolipid Pathway Metabolite Levels in the Plasma of Wild Type (WT) and *Agpat2*^{-/-} Mice.

Name	Males				Females			
	Plasma (pg/mg Protein)				Plasma (pg/mg Protein)			
	WT (n = 6)	<i>Agpat2</i> ^{-/-} (n = 6)	Fold Change	P Value	WT (n = 6)	<i>Agpat2</i> ^{-/-} (n = 6)	Fold Change	P Value
	Mean ± SD	Mean ± SD			Mean ± SD	Mean ± SD		
Sphinganine	5.23 ± 3.79	11.21 ± 6.54	2.14	0.09	5.09 ± 1.46	13.85 ± 6.01 ^a	2.72 ^c	0.01
Sphinganine 1P	170.68 ± 122.21	452.66 ± 230.57 ^a	2.65^d	0.03	140.26 ± 30.89	547.98 ± 135.79 ^a	3.91^d	<0.01
Deoxy sphinganine	ND	ND	ND	—	ND	ND	ND	—
DHC16:0	4.67 ± 2.79	8.70 ± 10.48	1.86	0.40	5.31 ± 1.22	6.38 ± 3.68	1.20	0.44
DHC18:0	4.05 ± 3.05	6.68 ± 3.98	1.65	0.23	5.51 ± 0.74	7.31 ± 1.40	1.33	0.07
DHC 24:0	8.54 ± 4.75	8.22 ± 7.97	-1.04	0.93	8.75 ± 2.06	7.74 ± 5.70	-1.13	0.87
DHC 24:1	17.07 ± 10.36	17.87 ± 15.80	1.05	0.92	17.11 ± 2.01	17.03 ± 7.57	1.00	0.91
SM 16:0	12031.24 ± 6861.02	9815.96 ± 3788.08 ^b	-1.23	0.50	13224.75 ± 2572.75	14732.00 ± 4583.52	1.11	0.50
SM 18:0	1000.23 ± 543.78	1748.32 ± 578.59 ^a	1.75 ^c	0.04	2242.75 ± 766.98	2744.98 ± 759.47	1.22	0.28
SM 24:0	6049.39 ± 3782.27	1820.08 ± 736.49 ^b	-3.32 ^c	0.04	4193.05 ± 1348.32	1847.55 ± 882.63 ^b	-2.27 ^c	<0.01
SM 24:1	18146.13 ± 9661.52	18393.44 ± 7812.37	1.01	0.96	22895.58 ± 8096.35	21529.06 ± 9774.50	-1.06	0.79
Cer16:0	24.64 ± 13.34	63.92 ± 15.52 ^a	2.59^d	0.01	25.95 ± 2.97	92.48 ± 5.90 ^a	3.56 ^d	<0.01
Cer18:0	5.20 ± 2.53	42.45 ± 11.07	8.16^d	<0.01	15.82 ± 4.47	76.82 ± 8.27 ^a	4.86 ^d	<0.01
Cer20:0	31.56 ± 16.35	25.38 ± 9.81	-1.24	0.44	13.93 ± 3.34	37.82 ± 10.27 ^a	2.72 ^c	<0.01
Cer22:0	344.94 ± 147.80	107.11 ± 44.79 ^b	-3.22 ^c	<0.01	89.52 ± 20.30	147.04 ± 60.39	1.64	0.14
Cer24:0	343.67 ± 6.04	171.79 ± 72.63 ^b	-2.00 ^c	0.04	218.36 ± 38.67	183.22 ± 75.24	-1.19	0.20
Cer24:1	373.76 ± 150.84	376.11 ± 169.36	1.01	0.98	264.99 ± 87.13	528.62 ± 179.40 ^a	1.99 ^c	0.04
HexCer-16:0	220.84 ± 166.50	269.99 ± 116.53	1.22	0.57	288.81 ± 68.12	432.24 ± 130.77	1.50	0.06
HexCer-18:0	28.73 ± 19.32	235.03 ± 126.93 ^a	8.18^d	0.01	263.47 ± 54.42	399.94 ± 55.60 ^a	1.52 ^d	<0.01
HexCer-22:0	2217.93 ± 1272.21	560.24 ± 292.83 ^a	-3.96 ^c	0.02	1052.80 ± 278.14	707.20 ± 336.13	-1.49	0.16
HexCer-24:1	771.82 ± 550.44	723.97 ± 447.56	-1.07	0.87	957.65 ± 347.43	914.02 ± 427.44	-1.05	0.89
LacCer-16:0	63.77 ± 41.29	36.59 ± 21.36	-1.74	0.19	28.01 ± 13.46	35.54 ± 22.78	1.27	0.60
LacCer-24:0	18.90 ± 9.09	11.69 ± 4.49	-1.62	0.12	11.48 ± 2.38	10.50 ± 3.83	-1.09	0.83
Sphingosine	7.44 ± 3.26	19.48 ± 8.80 ^a	2.62 ^c	0.02	7.29 ± 1.38	20.13 ± 7.20 ^a	2.76 ^c	<0.01
Sphingosine 1P	563.10 ± 284.93	799.13 ± 309.10	1.42	0.20	470.25 ± 76.75	927.75 ± 240.80 ^a	1.97 ^c	<0.01
Deoxy sphingosine	ND	ND	ND	—	ND	ND	ND	—

Shown are the mean ± SD, fold change, and *P* value for metabolites of the sphingolipid synthesis pathway in the plasma of *Agpat2*^{-/-} mice compared with those of WT mice.

Abbreviations: ND, not detected.

^aStatistically significant increases.

^bStatistically significant decreases.

^cStatistically significant increase in *Agpat2*^{-/-} mice when compared with WT.

^dIncreased in both liver and plasma of both sexes of *Agpat2*^{-/-} mice and are statistically significant. Those in bold represents significant increase in both sexes.

(*CerS6*^{bat-/-}) or in liver (*CerS*^{liver-/-}) resulted in improved glucose tolerance [25]. These previous studies and the current findings point to the notion that plasma ceramide levels reflect changes in hepatic ceramide levels and are valuable markers of hepatic metabolic health [27].

C. Increased Expression (Messenger RNA) of Enzymes Involved in Sphingolipid Biosynthesis in the Livers of 4-Month-Old *Agpat2*^{-/-} Mice

The elevated levels of liver sphingolipids correlate with an increase in the expression of the enzymes involved in sphingolipid biosynthesis. We measured the gene expression of key enzymes with the results shown in Fig. 2. Each of these enzymes has several isoforms except sphingosine-1-phosphate lyase (see Fig. 1). Although the increased gene expression is not as robust as observed for liver sphingolipid levels, in a steady state it is likely the metabolites accumulate over a period of time. The substrate specificities for some of these enzymes are now established (reviewed by Wegner et.al. [28]). For example, there are six different CerS, 1–6. Only CerS2 and CerS4–6 are expressed in the liver, and the increase in expression is in a range of one- to twofold. CerS2 prefers very long chain fatty acids to generate ceramide C22:0 to ceramide C24:0. This corresponds to an increased level of ceramide C24:1. CerS4 generally synthesizes ceramide with fatty acids C18:0 to C22:0, which we also see in the liver, whereas CerS5 and CerS6 prefer fatty

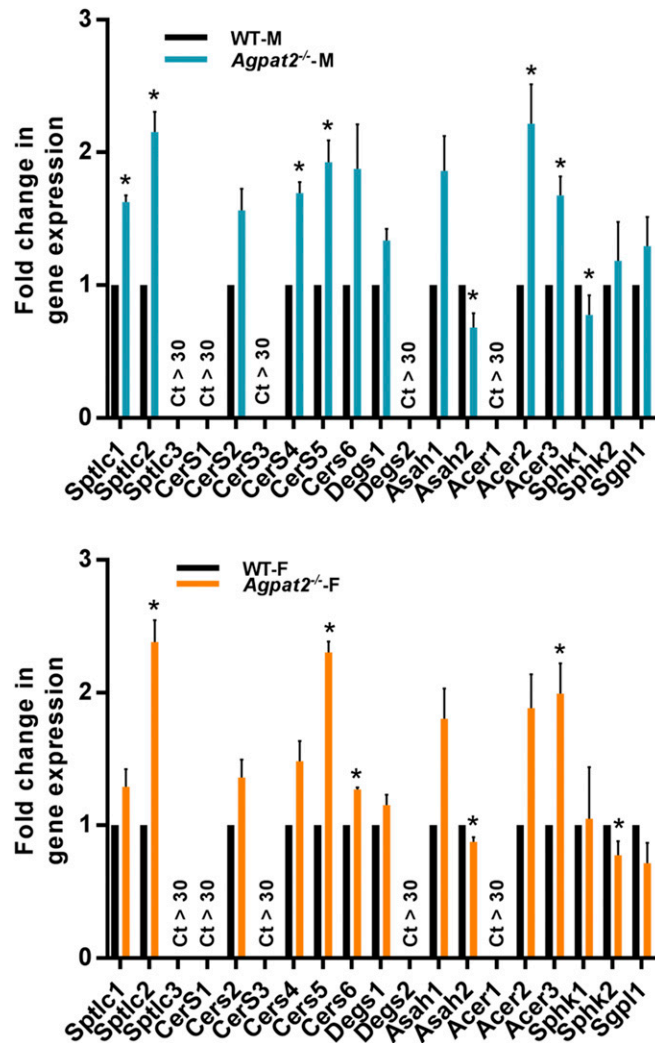


Figure 2. Hepatic expression of messenger RNA for enzymes of sphingolipid synthesis and metabolism. Expression of messenger RNA for *Sptlc1–3*, *CerS1–6*, *Dggs1–2*, *Asah1* (acid ceramidase), *Asah2* (nonlysosomal ceramidase), *Acer1–3* (alkaline ceramidase), *Sphk1–2*, and *Sgpl* (sphingosine 1-phosphate lyase) in the liver from WT and *Agpat2*^{-/-} male (upper panel) and female (lower panel) mice. Expression was analyzed by RT-qPCR and normalized to cyclophilin. Shown are the fold changes compared with WT liver (expressed as mean ± standard error of the mean, n = 3). Each measurement was carried out in pooled (n = 6) samples in duplicate and was considered as one sample. *P value ≤ 0.05. The expression of most of the enzymes for the sphingolipid synthesis and metabolism in the liver has been noted before (www.biogps.org) except those for *Sptlc2*, *Sptlc3*, *CerS1*, *CerS3*, *CerS4*, *CerS6*, *Dggs2*, *Asah2*, *Acer1*, *Acer3*, and *Sphk1*. Our data showed the expression of *Sptlc2*, *CerS4*, *CerS6*, *Asah2*, *Acer3*, and *Sphk1* genes in liver.

acid C16:0. The increased gene expression of these CerS correlates well with the observed elevated levels of the corresponding ceramide.

D. Ceramides Do Not Increase Glucose Output in Mouse Primary Hepatocytes Obtained From WT or *Agpat2*^{-/-} Mice

We next tested whether the ceramides, as those observed for PAs [9], also increase gluconeogenesis in hepatocytes. Among all the monitored ceramides, ceramide C16:0 and C18:0 were elevated in both sexes. Thus, we selected these two ceramides for our *in vitro* studies. Ceramide C24:1 was also included because this ceramide bears one unsaturation in the fatty

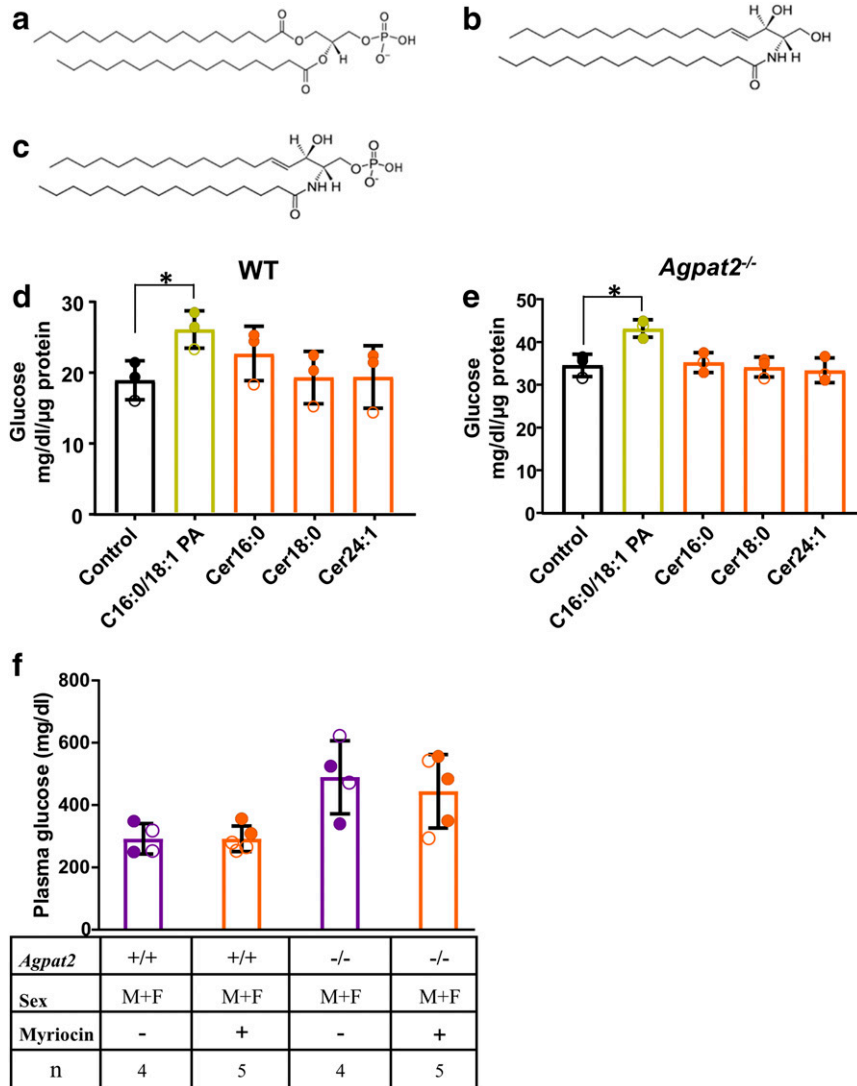


Figure 3. Glucose output remained unchanged in primary mouse hepatocytes in the presence of ceramide, and *Agpat2*^{-/-} mice do not show a decrease in plasma glucose levels upon administering myriocin, an inhibitor of ceramide synthesis. (a–c) A representative chemical structure of PA (C16:0/16:0) (a), ceramide (C16:0) (b), and ceramide 1-phosphate (C16:0) (c). Note a near structural similarity between PA and ceramide 1-phosphate. Glucose output was measured in the culture medium from the WT (d) and *Agpat2*^{-/-} (e) primary mouse hepatocytes, when tested with the following ceramides: C16:0, C18:0, and C24:1. Glucose is expressed as mg/dL/μg protein. C16:0/18:1 PA was included as a positive control. Bar represents mean ± standard error of the mean obtained from three independent experiments performed in duplicate. **P* value ≤ 0.05. (f) Shown are the individual plasma glucose levels in WT and *Agpat2*^{-/-} mice. For individual hepatocytes or *in vivo* experiments, either male or female mice were used. For analysis, the data from both the sexes were combined. Filled circles represent males, and unfilled circles represent females.

acid chain [Fig. 3(a–c)]. As shown in Fig. 3(d) and 3(e), when testing for glucose production in mouse primary hepatic cells, we observed an increase with C16:0/18:1 PA, as reported earlier [9], which was used in this study as a positive control, but no statistically significant increase with the above-mentioned ceramides was observed. This suggests that ceramides do not increase hepatic gluconeogenesis in cultured mouse primary hepatocytes. Because the chemical structures of PA and ceramide 1-phosphate are very similar [Fig. 3(a–c)], we also tested ceramide C16:0-1-phosphate for its ability to increase glucose output. Again, we did not see an increase in glucose output (n = 1, data not shown). We also tested the plasma glucose

levels in whole animals while administering the *Sptlc1* inhibitor myriocin and observed no decrease in plasma glucose level in *Agpat2*^{-/-} mice [Fig. 3(f)].

3. Discussion

The role of ceramide is widely established as an insulin desensitizer [29]. In this work, our goal was to determine whether ceramides also have any role in *de novo* hepatic glucose synthesis, and, as tested in mouse primary hepatocytes, they did not increase glucose production. It is interesting to note that chemical structures of PA and ceramides are similar but not identical. The lipids essentially differ in their skeletal backbone: PA has a glycerol backbone, whereas ceramide has a serine backbone group. This study further establishes the lipid specificity for the induction of hepatic glucose synthesis by PA, as reported earlier [9], but not by ceramides (this study) or other phospholipids reported earlier [9]. A previous study, reported that ceramide C2:0 (tested at 20–50 μM) increased glucose production from mouse primary hepatocytes [30]. However, in our study, we did not detect ceramide C2:0 in the livers of *Agpat2*^{-/-} mice. These investigators also showed that intraperitoneal administration of ceramide C16:0 (10 mg/kg/d for 1 week) resulted in glucose intolerance in intestine-specific farnesoid X receptor knockout (*Fxr*^{ΔIE}) mice [30]. However, our data show no effects of ceramide C16:0, as well as C18:0 and C24:1 (the predominant ceramide species in the livers of *Agpat2*^{-/-} mice) on glucose output from mouse primary hepatocytes.

Another interesting observation is the increased plasma levels of ceramides in *Agpat2*^{-/-} mice. Although not studied directly, it has been widely reported that some of the ceramides could be secreted as part of very-low-density lipoprotein secretion from the liver [31]. Additionally, as demonstrated in cultured HepG2 cells, increased hepatic ceramide levels resulted in increased secretion of liver ceramides [32]. It has been a long-standing goal to identify plasma biomarkers for the development of type 2 diabetes (reviewed in [27]). In a recent study, it was reported that plasma sphingolipids were increased in nonhuman primates fed a Western-style diet [33], specifically the molecular species of ceramide C14:0, C16:0, C22:0, and C24:0, which correlated well with insulin resistance. In another study, ceramide C22:0 was also increased in obese female children and adolescents with type 2 diabetes [34]. Ceramides C16:0 and C22:0 were also found to be elevated in the current study. Thus, it seems that these studies corroborate the increased plasma levels of ceramides C16:0 and C22:0 in type 2 and lipodystrophic diabetes.

Does the activation of the sphingolipid synthesis pathway have any additional function(s)? The livers of *Agpat2*^{-/-} mice have elevated fatty acid synthesis [2] and phospholipids [2] despite the fact that the main route for its synthesis is genetically deleted and the total AGPAT enzymatic activity remains ~10% of the WT mice. We have shown that conversion of diacylglycerol to PA by diacylglycerol kinase can occur in the livers of *Agpat2*^{-/-} mice [9]. It is also possible that the downstream product of ceramide, sphingosine 1-phosphate, might provide an additional substrate for synthesis of phospholipids as a first step in converting sphingolipids to phospholipids [35]. The enzymes for these conversions have recently been identified in yeast [36] and in *Drosophila* [37] (reviewed in [38]) (see Fig. 4). The enzyme, sphingosine 1-phosphate lyase (*Sgpl1*), which synthesizes hexadecenal and ethanolamine-phosphate, is present in the livers of mice. Although the messenger RNA expression of *Sgpl1* in this study did not increase in the *Agpat2*^{-/-} mice compared with the WT mice, this does not necessarily mean that *Sgpl1* has no function in synthesizing phospholipid from sphingosine. In a steady state condition, it might result in this conversion, albeit at a very low rate. In fact, a decrease in phosphatidylethanolamine and phosphatidylserine in the livers of *Sgpl1*^{-/-} mice has been reported [39]. Additional experiments are needed to determine whether this route for the synthesis of phospholipids in the livers of *Agpat2*^{-/-} mice is functional.

As mentioned above, an increased *de novo* lipogenesis in the livers of *Agpat2*^{-/-} mice [2] and the disruption of hepatic phospholipid synthesis might shift the equilibrium of fatty acids toward their usage in the sphingolipid synthesis pathway. Although this study shows that when ceramide was tested in isolated hepatocytes it did not increase hepatic gluconeogenesis,

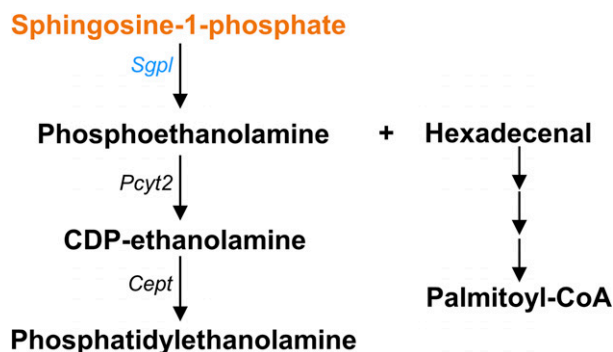


Figure 4. Pathway for conversion of sphingosine to glycerophospholipid. The generation of sphingosine 1-phosphate is shown in Fig. 1. The enzyme sphingosine 1-phosphate lyase cleaves sphingosine 1-phosphate to generate phosphoethanolamine and hexadecenal. As shown, both the molecules trace two independent pathways. Phosphoethanolamine is converted to CDP-ethanolamine, followed by its sequential conversion to phosphatidylethanolamine. Hexadecenal enters the route to be converted to palmitoyl-coenzyme A via a series of intermediate steps, and could then re-enter the sphingolipid synthesis pathway. *Sgpl*, Sphingosine 1-phosphate lyase; *Pcyt2*, phosphoethanolamine cytidyltransferase; and *Cept*, cytidine 5'-diphosphate-ethanolamine phosphotransferase. The metabolites shown in orange and the enzymes shown in blue were measured in this study.

future studies will reveal the role of other sphingolipids in gluconeogenesis. We have previously demonstrated that, despite the deficiency of one of the *Agpats*, *Agpat2*, which results in ~90% decrease in the hepatic enzymatic activity [2], the PA levels were not decreased. This is a result of hepatic upregulation of diacylglycerol kinase [9]. Therefore, previous and current studies suggest additional experimental undertaking in resolving the role of each of the sphingolipid metabolite(s) of this pathway for hepatic gluconeogenesis.

In summary, we have shown that the entire pathway for sphingolipid synthesis is activated for both the expression of respective enzymes and the associated metabolites. This study further determined the specificity of PA (reported earlier [9]) toward increasing glucose output from primary hepatocytes since tested ceramides did not increase the hepatic glucose output. Lastly, we can speculate from this study that increased hepatic sphingosine 1-phosphate and the enzyme *Sgpl1* might divert some of it toward the synthesis of phospholipids. However, this needs further confirmation.

Acknowledgments

We thank Katie Tunison for copy editing, and Ruth Gordillo, Philipp Scherer, and Jay Horton from the Metabolic Core Facility for measuring sphingolipids.

Address all correspondence to: Anil K. Agarwal, PhD, Division of Nutrition and Metabolic Diseases, Department of Internal Medicine, University of Texas Southwestern Medical Center, Dallas, Texas 75390. E-mail: Anil.Agarwal@utsouthwestern.edu.

This work was supported by National Institutes of Health Grant R01-DK54387 and the Southwest Medical Foundation.

Author contributions: A.K.A. conceived the study. Methodology, validation, visualization, formal analysis, and investigation were performed by S.S. and A.K.A. Original draft preparation and supervision were conducted by A.K.A. S.S., A.G., and A.K.A. reviewed and edited the paper. A.G. and A.K.A. acquired funding.

Disclosure Summary: The authors have nothing to disclose.

References and Notes

1. Agarwal AK, Arioglu E, De Almeida S, Akkoc N, Taylor SI, Bowcock AM, Barnes RI, Garg A. AGPAT2 is mutated in congenital generalized lipodystrophy linked to chromosome 9q34. *Nat Genet.* 2002;**31**(1):21–23.

2. Cortés VA, Curtis DE, Sukumaran S, Shao X, Parameswara V, Rashid S, Smith AR, Ren J, Esser V, Hammer RE, Agarwal AK, Horton JD, Garg A. Molecular mechanisms of hepatic steatosis and insulin resistance in the AGPAT2-deficient mouse model of congenital generalized lipodystrophy. *Cell Metab.* 2009;**9**(2):165–176.
3. Agarwal AK, Sukumaran S, Cortés VA, Tunison K, Mizrahi D, Sankella S, Gerard RD, Horton JD, Garg A. Human 1-acylglycerol-3-phosphate O-acyltransferase isoforms 1 and 2: biochemical characterization and inability to rescue hepatic steatosis in Agpat2(-/-) gene lipodystrophic mice. *J Biol Chem.* 2011;**286**(43):37676–37691.
4. Agarwal AK. Lysophospholipid acyltransferases: 1-acylglycerol-3-phosphate O-acyltransferases: from discovery to disease. *Curr Opin Lipidol.* 2012;**23**(4):290–302.
5. Sukumaran S, Barnes RI, Garg A, Agarwal AK. Functional characterization of the human 1-acylglycerol-3-phosphate-O-acyltransferase isoform 10/glycerol-3-phosphate acyltransferase isoform 3. *J Mol Endocrinol.* 2009;**42**(6):469–478.
6. Cao J, Liu Y, Lockwood J, Burn P, Shi Y. A novel cardiolipin-remodeling pathway revealed by a gene encoding an endoplasmic reticulum-associated acyl-CoA:lysocardiolipin acyltransferase (ALCAT1) in mouse. *J Biol Chem.* 2004;**279**(30):31727–31734.
7. Zhao Y, Chen YQ, Li S, Konrad RJ, Cao G. The microsomal cardiolipin remodeling enzyme acyl-CoA lysocardiolipin acyltransferase is an acyltransferase of multiple anionic lysophospholipids. *J Lipid Res.* 2009;**50**(5):945–956.
8. Harayama T, Shindou H, Ogasawara R, Suwabe A, Shimizu T. Identification of a novel non-inflammatory biosynthetic pathway of platelet-activating factor. *J Biol Chem.* 2008;**283**(17):11097–11106.
9. Sankella S, Garg A, Horton JD, Agarwal AK. Hepatic gluconeogenesis is enhanced by phosphatidic acid which remains uninhibited by insulin in lipodystrophic Agpat2(-/-) mice. *J Biol Chem.* 2014;**289**(8):4762–4777.
10. Yetukuri L, Katajamaa M, Medina-Gomez G, Seppänen-Laakso T, Vidal-Puig A, Oresic M. Bioinformatics strategies for lipidomics analysis: characterization of obesity related hepatic steatosis. *BMC Syst Biol.* 2007;**1**:12.
11. Sajan MP, Ivey RA, Lee MC, Farese RV. Hepatic insulin resistance in ob/ob mice involves increases in ceramide, aPKC activity, and selective impairment of Akt-dependent FoxO1 phosphorylation. *J Lipid Res.* 2015;**56**(1):70–80.
12. Chen W, Zhou H, Saha P, Li L, Chan L. Molecular mechanisms underlying fasting modulated liver insulin sensitivity and metabolism in male lipodystrophic Bslc2/Seipin-deficient mice. *Endocrinology.* 2014;**155**(11):4215–4225.
13. Baenke F, Peck B, Miess H, Schulze A. Hooked on fat: the role of lipid synthesis in cancer metabolism and tumour development. *Dis Model Mech.* 2013;**6**(6):1353–1363.
14. Hannun YA, Obeid LM. Principles of bioactive lipid signalling: lessons from sphingolipids. *Nat Rev Mol Cell Biol.* 2008;**9**(2):139–150.
15. Merrill AH, Jr. De novo sphingolipid biosynthesis: a necessary, but dangerous, pathway. *J Biol Chem.* 2002;**277**(29):25843–25846.
16. Li Z, Li Y, Chakraborty M, Fan Y, Bui HH, Peake DA, Kuo MS, Xiao X, Cao G, Jiang XC. Liver-specific deficiency of serine palmitoyltransferase subunit 2 decreases plasma sphingomyelin and increases apolipoprotein E levels. *J Biol Chem.* 2009;**284**(39):27010–27019.
17. Mitsnefes M, Scherer PE, Friedman LA, Gordillo R, Furth S, Warady BA; CKiD Study Group. Ceramides and cardiac function in children with chronic kidney disease. *Pediatr Nephrol.* 2014;**29**(3):415–422.
18. Hammad SM, Pierce JS, Soodavar F, Smith KJ, Al Gadban MM, Rembiesa B, Klein RL, Hannun YA, Bielawski J, Bielawska A. Blood sphingolipidomics in healthy humans: impact of sample collection methodology. *J Lipid Res.* 2010;**51**(10):3074–3087.
19. Shaner RL, Allegood JC, Park H, Wang E, Kelly S, Haynes CA, Sullards MC, Merrill AH, Jr. Quantitative analysis of sphingolipids for lipidomics using triple quadrupole and quadrupole linear ion trap mass spectrometers. *J Lipid Res.* 2009;**50**(8):1692–1707.
20. Shimomura I, Bashmakov Y, Ikemoto S, Horton JD, Brown MS, Goldstein JL. Insulin selectively increases SREBP-1c mRNA in the livers of rats with streptozotocin-induced diabetes. *Proc Natl Acad Sci USA.* 1999;**96**(24):13656–13661.
21. Matsuda M, Korn BS, Hammer RE, Moon YA, Komuro R, Horton JD, Goldstein JL, Brown MS, Shimomura I. SREBP cleavage-activating protein (SCAP) is required for increased lipid synthesis in liver induced by cholesterol deprivation and insulin elevation. *Genes Dev.* 2001;**15**(10):1206–1216.
22. Spandidos A, Wang X, Wang H, Seed B. PrimerBank: a resource of human and mouse PCR primer pairs for gene expression detection and quantification. *Nucleic Acids Res.* 2010;**38**(Database issue):D792–D799.

23. Spandidos A, Wang X, Wang H, Dragnev S, Thurber T, Seed B. A comprehensive collection of experimentally validated primers for polymerase chain reaction quantitation of murine transcript abundance. *BMC Genomics*. 2008;**9**:633.
24. Wang X, Seed B. A PCR primer bank for quantitative gene expression analysis. *Nucleic Acids Res*. 2003;**31**(24):e154.
25. Turpin SM, Nicholls HT, Willmes DM, Mourier A, Brodesser S, Wunderlich CM, Mauer J, Xu E, Hammerschmidt P, Brönneke HS, Trifunovic A, LoSasso G, Wunderlich FT, Kornfeld JW, Blüher M, Krönke M, Brüning JC. Obesity-induced CerS6-dependent C16:0 ceramide production promotes weight gain and glucose intolerance. *Cell Metab*. 2014;**20**(4):678–686.
26. Raichur S, Wang ST, Chan PW, Li Y, Ching J, Chaurasia B, Dogra S, Öhman MK, Takeda K, Sugii S, Pewzner-Jung Y, Futerman AH, Summers SA. CerS2 haploinsufficiency inhibits β -oxidation and confers susceptibility to diet-induced steatohepatitis and insulin resistance [published correction appears in *Cell Metab*. 2014;**20**(5):919]. *Cell Metab*. 2014;**20**(4):687–695.
27. Xia JY, Morley TS, Scherer PE. The adipokine/ceramide axis: key aspects of insulin sensitization. *Biochimie*. 2014;**96**:130–139.
28. Wegner MS, Schiffmann S, Parnham MJ, Geisslinger G, Grösch S. The enigma of ceramide synthase regulation in mammalian cells. *Prog Lipid Res*. 2016;**63**:93–119.
29. Chaurasia B, Summers SA. Ceramides: lipotoxic inducers of metabolic disorders. *Trends Endocrinol Metab*. 2015;**26**(10):538–550.
30. Xie C, Jiang C, Shi J, Gao X, Sun D, Sun L, Wang T, Takahashi S, Anitha M, Krausz KW, Patterson AD, Gonzalez FJ. An intestinal farnesoid X receptor-ceramide signaling axis modulates hepatic gluconeogenesis in mice. *Diabetes*. 2017;**66**(3):613–626.
31. Boon J, Hoy AJ, Stark R, Brown RD, Meex RC, Henstridge DC, Schenk S, Meikle PJ, Horowitz JF, Kingwell BA, Bruce CR, Watt MJ. Ceramides contained in LDL are elevated in type 2 diabetes and promote inflammation and skeletal muscle insulin resistance. *Diabetes*. 2013;**62**(2):401–410.
32. Watt MJ, Barnett AC, Bruce CR, Schenk S, Horowitz JF, Hoy AJ. Regulation of plasma ceramide levels with fatty acid oversupply: evidence that the liver detects and secretes de novo synthesized ceramide. *Diabetologia*. 2012;**55**(10):2741–2746.
33. Brozinick JT, Hawkins E, Hoang Bui H, Kuo MS, Tan B, Kievit P, Grove K. Plasma sphingolipids are biomarkers of metabolic syndrome in non-human primates maintained on a Western-style diet. *Int J Obes*. 2013;**37**(8):1064–1070.
34. Lopez X, Goldfine AB, Holland WL, Gordillo R, Scherer PE. Plasma ceramides are elevated in female children and adolescents with type 2 diabetes. *J Pediatr Endocrinol Metab*. 2013;**26**(9–10):995–998.
35. Gerl MJ, Bittl V, Kirchner S, Sachsenheimer T, Brunner HL, Luchtenborg C, Özbalci C, Wiedemann H, Wegehingel S, Nickel W, Haberkant P, Schultz C, Krüger M, Brügger B. Sphingosine-1-phosphate lyase deficient cells as a tool to study protein lipid interactions. *PLoS One*. 2016;**11**(4):e0153009.
36. Nakahara K, Ohkuni A, Kitamura T, Abe K, Naganuma T, Ohno Y, Zoeller RA, Kihara A. The Sjögren-Larsson syndrome gene encodes a hexadecenal dehydrogenase of the sphingosine 1-phosphate degradation pathway. *Mol Cell*. 2012;**46**(4):461–471.
37. Dobrosotskaya IY, Seegmiller AC, Brown MS, Goldstein JL, Rawson RB. Regulation of SREBP processing and membrane lipid production by phospholipids in *Drosophila*. *Science*. 2002;**296**(5569):879–883.
38. Pulkoski-Gross MJ, Donaldson JC, Obeid LM. Sphingosine-1-phosphate metabolism: a structural perspective. *Crit Rev Biochem Mol Biol*. 2015;**50**(4):298–313.
39. Bektas M, Allende ML, Lee BG, Chen W, Amar MJ, Remaley AT, Saba JD, Proia RL. Sphingosine 1-phosphate lyase deficiency disrupts lipid homeostasis in liver. *J Biol Chem*. 2010;**285**(14):10880–10889.